Polymer Electrolyte Membranes Based on Multiblock Poly(phenylene ether ketone)s with Pendant Alkylsulfonic Acids: Effects on the Isomeric Configuration and Ion Transport Mechanism

ARTICLE *in* THE JOURNAL OF PHYSICAL CHEMISTRY C · AUGUST 2015

Impact Factor: 4.77 · DOI: 10.1021/acs.jpcc.5b04480

THE JOURNAL OF PHYSICAL CHEMISTRY C

Article

pubs.acs.org/JPCC

Polymer Electrolyte Membranes Based on Multiblock Poly(phenylene ether ketone)s with Pendant Alkylsulfonic Acids: Effects on the Isomeric Configuration and Ion Transport Mechanism

Xuan Zhang,*[,†] Tiandu Dong,[†] Yanli Pu,[‡] Tomoya Higashihara,[§] Mitsuru Ueda,*[,§] and Lianjun Wang*[,†]

[†]Key Laboratory of Jiangsu Province for Chemical Pollution Control and Resources Reuse, Nanjing University of Science & Technology, 200 Xiaolingwei, Nanjing 210094, Jiangsu Province, China

[‡]Center for Disease Prevention and Control, 9 Huangshan South Road, Zhenjiang 212004, Jiangsu Province, China

[§]Department of Polymer Science and Engineering, Faculty of Engineering, Yamagata University, 4-3-16 Jonan, Yonezawa City, Yamagata 992-8510, Japan

Supporting Information

ABSTRACT: Two structural variations of multiblock poly(phenylene ether ketone)s (bSPPEKs) with pendant alkylsulfonic acids were prepared by a polycondensation reaction between oligomeric difluoro and diphenoxide precursors, followed by successive demethylation and sulfonation processes. Two isomers, bis[4-fluoro-3-(4′-methoxylbenzoyl)]biphenyl (*p*-BFMBP) and bis[5-fluoro-2-(4′-methoxylbenzoyl)]-biphenyl (*m*-BFMBP), were prepared as the difluoro starting monomers. The corresponding polymer membranes were obtained with good mechanical stability to facilitate the further characterizations. The morphology of bSPPEKs was confirmed by atomic force microscopy, from which the distinct phase separation could be identified with the average hydrophilic domain size of ca. 15−20 nm for the *m*-bSPPEKs. It is worth noting that both *m*- and *p*-bSPPEKs show quite comparable, or even better, ion conduction capacities than commercially available Nafion membrane, especially under low relative humidity conditions (30−50%), suggesting their promising future as polymer electrolyte membrane candidates. Meanwhile, the proton conductivities of all of the *m*-bSPPEKs were found to be greater than those of the *p*-bSPPEKs over the entire relative humidity range, indicating better water-retention capacity and lower resistance to the ion transport. In addition, molecular dynamics simulation was employed to extensively explore the structure−property relationship between the two polymers. The length, angle, and torsion distribution results clearly reveal their steric configurations, that is, a longer length and smaller angle in the side chain, together with a smaller torsion angle in the main chain for *m*-bSPPEKs, which produces slightly more free volume inside the polymer matrix. Analysis of the diffusion coefficients and coordination numbers shows that there is more water clustering around the sulfonic acid groups in the meta-polymers than in the para-polymers.

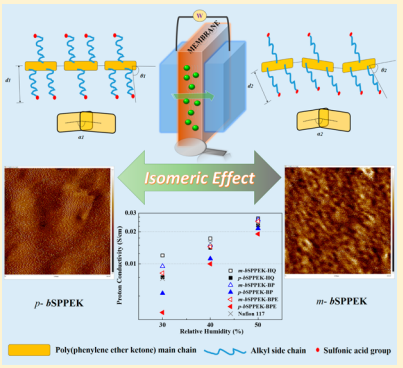

INTRODUCTION

Fuel-cell systems are highly promising electrochemical devices for various future applications. These systems rely on the performance of polymer electrolyte membranes (PEMs) as separators. The devices function only when the membranes can efficiently separate the electrodes and mediate the electrochemical reactions at the anode and cathode by ion conduction.[1−4] In general, ion-conducting membranes are of two major types according to the polymer backbones, fluorinated and aromatic ionomers. For instance, Nafion (DuPont), Flemion (Asahi Glass), and Aquivion (Solvay Solex Company) are typical perfluorosulfonic acid membranes (PFSA).[5,6] Examples of typical aromatic membranes are sulfonated poly(arylene ether sulfone),[7,8] sulfonated poly(arylene ether ketone),[9,10] sulfonated polyphenylene,[11−13] and so on. PEM technologies have been extensively studied for nearly 20 years, and the research focus has now shifted to the development of novel polymeric materials and improvement of existing materials through various modifications.

Despite the large number of reports on new and improved polymer membranes, it is difficult to perform a comprehensive comparison of the different polymer types. Even a slight change in the polymer structures, for example, architectures (random,[14,15] block,[16,17] graft,[18,19] etc.) or chain types (main chain,[20,21] side chain,[22,23] etc.), would have a significant influence on the final performance of the membrane. For instance, our group previously reported a series of sulfonated poly(phenylene ether)s (SPPEs).[24] A difluoro-functional monomer, bis[4-fluoro-3-(4′-methoxylbenzoyl)]biphenyl (*p*-BFMBP), was polymerized with various bisphenols, (i.e., hydroquinone (HQ), 4,4′-biphenol (BP), and 4,4′-oxidiphenol

Received: May 10, 2015
Revised: June 27, 2015
Published: August 7, 2015

DOI: 10.1021/acs.jpcc.5b04480
J. Phys. Chem. C 2015, 119, 19596−19606

(BPE)), to obtain AB-type copolymers. The three polymers thus prepared possessed similar structures, yet they exhibited considerably different properties. In particular, a significant improvement was observed in the mechanical strength and proton conductivity of the polymers when a certain number of "ether" linkages were introduced into the polymer backbones.

However, because of the very small repeating units, all of the membranes did not show good phase separation. The hydrophilic domains were all isolated and surrounded by the hydrophobic ones, as evidenced by their atomic force microscopy (AFM) pictures. The only apparent way to improve the conductivity performance would be to increase the degree of sulfonation (DS) during our experimental process, and this would inevitably involve some other negative effects, such as the dramatic swelling, which might be the biggest challenge for practical application of those membranes. Therefore, it is quite necessary to approval some changes on the polymer chain types, for example, a multiblock architecture, as a very effective way to control the DS with maintaining the good phase separation to support the ion exchange.[8,16,17]

Additionally, considering the importance of the selection of appropriate membrane materials and their potential market value, it is essential to obtain information on the structure-performance relationship so as to understand the fundamental properties of the materials themselves. Recently, the molecular dynamics simulation (MDS) method has been applied to investigate the "molecular world" based on quantum chemistry principles and thus has drawn much attention.[25−30] For instance, a comparison study was performed among the 3 M membranes based on different equivalent weights (EWs). The larger crystalline domains present in the higher EW membranes were found to reduce the probability of charge transfer along the interface.[25] In another related study, Voth et al. comprehensively stimulated the proton transport in 3 M and Nafion membranes and found that the calculated self-diffusion constants of the excess protons were slightly higher for the former.[26] Furthermore, hydrated morphological studies of PFSA membranes were carried out by a mesoscopic simulation, from which the water domains could be clearly distinguished;[27] however, most of the current research studies are focused on the PFSA ionomers, and the information on aromatic polymers is still rather limited.

Clearly, there is a need for understanding the nature of materials by a simulation method, which can connect realistic membrane properties with the correct physics principles guiding the proton transport process to assist in improved PEM designs and advance fuel-cell research. Herein, we focus on the structure−property relationships in two structural variations of multiblock sulfonated poly(phenylene ether ketone)s using a couple of isomers as the starting monomers (Figure 1). Because the chemical compositions of the bSPPEKs were exactly the same, any possible discrepancies in their performances were systematically evaluated and compared by measuring their water uptake, mechanical properties, proton conductivity as well as their morphology. Furthermore, a purposeful simulation method was used to investigate the influence of the steric configurations of the polymers on a molecular level.

EXPERIMENTAL SECTION

Materials. 2-Chloro-4-fluorobenzoic acid, anisole, and $AlCl_3$ were purchased from TCI and used as received. Thionyl chloride was purchased from Wako Pure Chemical Industries

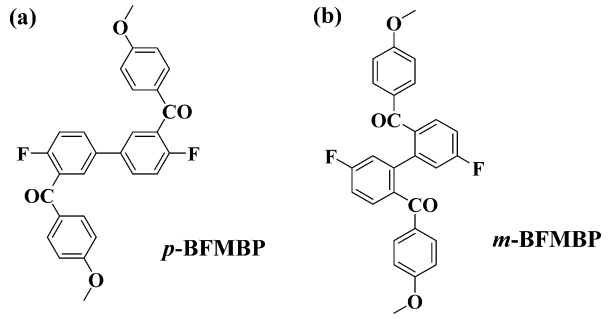

Figure 1. Chemical formulas of *p*-BFMBP and *m*-BFMBP.

and used as received. Bis(triphenylphosphino)nickel(II) (Ni-$(PPh_3)_2Cl_2$, TCI) was dried at 100 °C under vacuum prior to use. Zinc power was purchased from Aldrich, washed with 2.0 M hydrochloric acid, deionized water, ethanol, and diethyl ether, successively, and dried at 100 °C for 6 h under vacuum. *N*,*N*-Dimethylacetamide (DMAc, Wako) was dried over CaH_2, distilled under reduced pressure, and stored over 4 Å molecular sieves prior to use. Other solvents and reagents were used as received. Bis[4-fluoro-3-(4′-methoxylbenzoyl)]biphenyl (*p*-BFMBP) was synthesized according to our previous report.[24] The synthetic procedure on bis[5-fluoro-2-(4′-methoxylbenzoyl)]biphenyl (*m*-BFMBP) is presented in the Supporting Information.

Synthetic procedure of polymers. *Synthesis of Multiblock Poly(phenylene ether ketone)-OMe (P3).* A series of hydrophobic oligomers O1 (fluoro-terminated) was synthesized with controlled molecular weights. A typical procedure is as follows: 3.000 g (6.544 mmol) of *m*-BFMBP, 1.108 g (5.949 mmol) of BP, and 0.9870 g (7.139 mmol) of potassium carbonate were charged to a three-necked 100 mL flask equipped with a condenser, a Dean−Stark trap, a nitrogen inlet and outlet. Then, the fresh DMAc (21.0 mL) and toluene (10.0 mL) were added to the flask, and the reaction was heated to 140 °C with stirring until the toluene azeotropically removed the water in the system. After 4 h, the reaction was slowly increasing the temperature to 165 °C and allowed to proceed for another 4 h. The resulting viscous solution was cooled to room temperature and diluted with DMAc to facilitate filtration. After washing with water, the powder was thoroughly extracted with isopropyl alcohol (IPA) by a Soxhlet extractor. Finally, the grayish powder was dried at 80 °C in vacuo to afford a yield of 95%. The calculated block length from ^{1}H NMR was estimated to 10.

A series of hydrophobic oligomers O2 (phenoxide-terminated) was synthesized with controlled molecular weights. A typical procedure as follows: 3.000 g (13.75 mmol) of 4,4′-difluorobenzophenone, 2.816 g (15.12 mmol) of BP, and 2.436 g (18.15 mmol) of potassium carbonate were charged to a three-necked 100 mL flask equipped with a condenser, a Dean−Stark trap, a nitrogen inlet, and outlet. Then, the fresh DMAc (29.0 mL) and toluene (15.0 mL) were added to the flask, and the reaction was heated to 140 °C with stirring until the toluene azeotropically removed the water in the system. After 4 h, the reaction was slowly increasing the temperature to 165 °C and allowed to proceed for another 4 h. The resulting viscous solution was cooled to room temperature and diluted with DMAc to facilitate filtration. After washing with water, the powder was thoroughly extracted with IPA by a Soxhlet extractor. Finally, the white powder was dried at 80 °C in vacuo

DOI: 10.1021/acs.jpcc.5b04480
J. Phys. Chem. C 2015, 119, 19596−19606

Scheme 1. Synthesis of *m*- or *p*-bPPEK (P3): (a) Hydroquinone (HQ), (b) 4,4′-Biphenol (BP), and (c) 4,4′-Oxidiphenol (BPE)

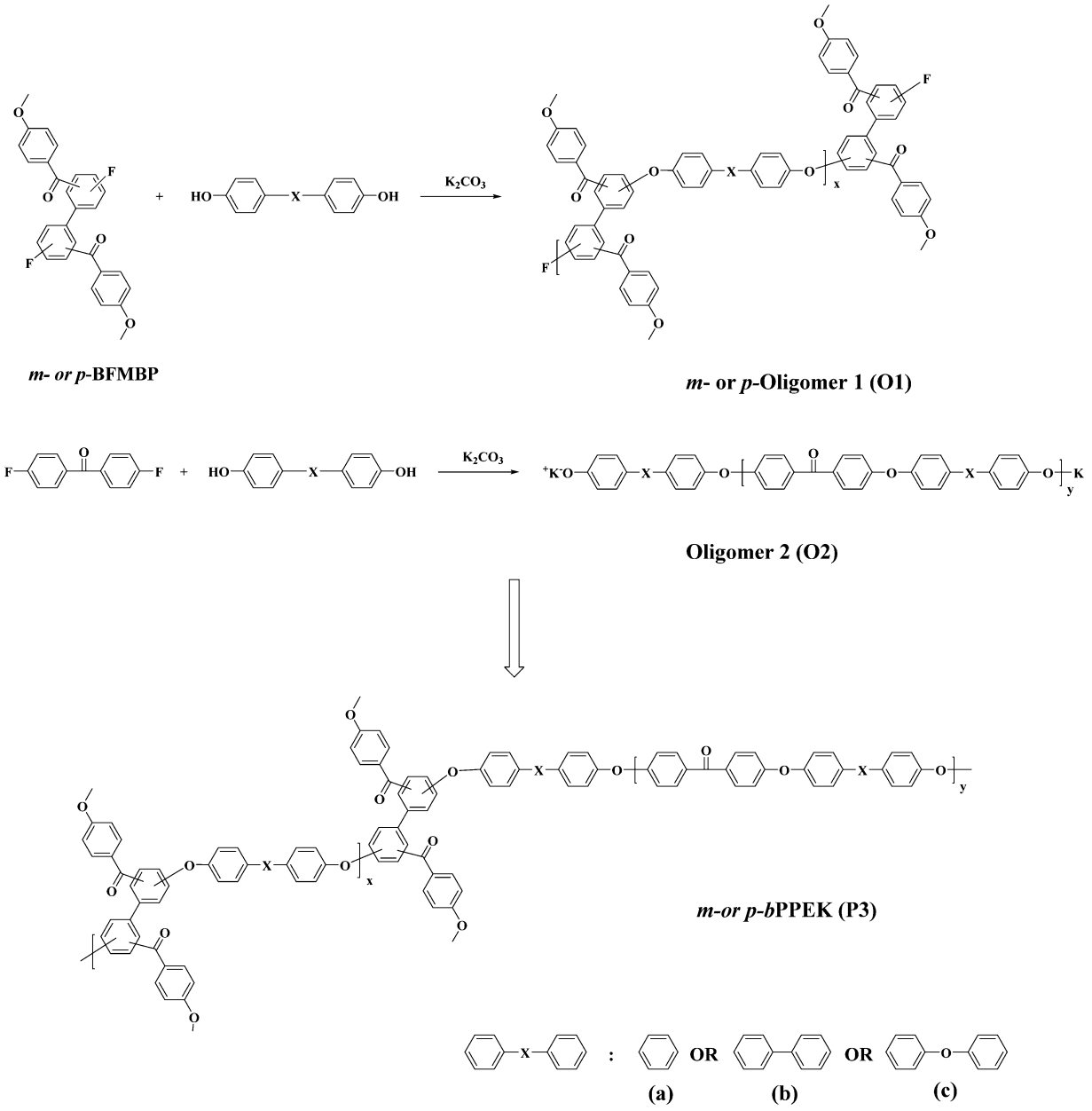

to afford a yield of 91%. The calculated block length from ^{1}H NMR was estimated to 10.

Three series of multiblock copolymers P3 with different bisphenol type were synthesized via a polycondensation reaction between fluoro-terminated oligomer O1 and phenoxide-terminated oligomers O2. A typical procedure for P3 (BP type) was performed as follows: 1.696 g (0.260 mmol) of O1, 1.000 g (0.260 mmol) of O2, 0.043 g (0.312 mmol) of potassium carbonate, 17.0 mL of DMAc, and 10.0 mL of cyclohexane were added to a three-necked 100 mL flask equipped with a condenser, a Dean−Stark trap, a nitrogen inlet, and outlet. The reaction mixture was heated to 90 °C for 4 h to dehydrate the system with refluxing cyclohexane. After removing the cyclohexane, the coupling reaction was conducted at 110 °C for 8 h. The resulting yellowish polymer solution was precipitated in water. The fiber-like copolymer was purified in a Soxhlet extractor with IPA for 24 h for another 24 h and dried at 80 °C in vacuo to afford a yield of 92%. FTIR (KBr): ν 2960−2870 (C−H), 1658 (C═O), 1597 (C═C), 1169 cm^{-1} (C−O−C). ^{1}H NMR (DMSO-d_6): δ = 7.76−6.78 (*bm*, Ar−H), δ = 3.68 (*s*, −OCH$_3$).

Synthesis of Multiblock Poly(phenylene ether ketone)−OH (P4). A typical synthetic procedure of P4 (BP type) is as follows. To a 100 mL three-necked flask equipped with a nitrogen inlet/outlet were charged P3 (BP type) (1.000 g, 2.130 mmol) and CH_2Cl_2 (20.0 mL). The solution was cooled to 0 °C in an ice bath, and a BBr_3/CH_2Cl_2 solution (10.7 mL) was added dropwise to the solution. After addition, the reaction was kept at room temperature overnight. The resulting copolymer was obtained by carefully pouring the solution into water, filtered, washed thoroughly with water and methanol, successively, and dried under vacuum at 80 °C for 12 h. Yield: 0.950 g (98%). FTIR (KBr): ν 2960−2870 (C−H), 1658 (C═O), 1597 (C═C), 1169 cm^{-1} (C−O−C). ^{1}H NMR (DMSO-d_6): δ = 10.34 (*bs*, −OH), δ = 7.77−6.66 (*bm*, Ar−H).

DOI: 10.1021/acs.jpcc.5b04480
J. Phys. Chem. C 2015, 119, 19596−19606

Synthesis of Sulfonated Multiblock Poly(phenylene ether ketone) (P5). A typical synthetic procedure of P5 (BP type) is as follows. To a 20 mL three-necked flask equipped with a nitrogen inlet/outlet were charged P4 (BP type) (0.800 g, 1.765 mmol), sodium hydride (0.063 g, 2.648 mmol), and dimethyl sulfoxide (DMSO) (16.0 mL). The solution was heated to 100 °C, and 1,4-butane sultone (0.481 g, 3.530 mmol) was added dropwise to the mixture. After 12 h, the solution was cooled to room temperature and slowly poured in EtOH. The sulfonated copolymer was thoroughly washed by water and EtOH and then dried in a vacuum oven at 80 °C for 24 h. Yield: 0.936 g (90%). FTIR (KBr): ν 2960−2870 (C−H), 1658 (C═O), 1600 (C═C), 1176 (C−O−C), 1119, 1049 cm^{-1} (O═S═O). ^{1}H NMR (DMSO-d_6): δ = 7.79−6.83 (*bm*, Ar−H), δ = 3.95 (*bs*, -OCH_2−), δ = 2.60 (*bs*, −CH_2−SO_3Na), δ = 1.74 (*bs*, −CH_2−).

Preparation of P5 Membranes. Membranes were prepared by a solution-casting method. P5 was dissolved in DMSO with concentration of 10% (m/v). After filtration, the solution was cast onto a clean Petri dish, dried at 80 °C for 20 h under atmosphere. The membrane was detached from the dish by immersing into water to remove the residual solvent, followed by soaking in 2 M HCl (aq) at 50 °C for 72 h for proton exchange. Then, the membrane was thoroughly washed with Milli-Q water. The thickness of the membranes was controlled to be ∼50 μm.

Characterizations. ^{1}H and ^{13}C NMR spectra were recorded on a Bruker AVANCE III 500 MHz spectrometer using $CDCl_3$ or DMSO-d_6 as the solvent and tetramethylsilane as the reference. Fourier transform-infrared (FT-IR) spectra were obtained with a Horiba FT-120 Fourier transform spectrophotometer. Number- and weight-average molecular weights (M_n and M_w) were measured by gel permeation chromatography (GPC) on a Hitachi LC-7000 system equipped with polystyrene gel columns (TSKgel GMHHR-M) eluted with *N*,*N*-dimethylformamide (DMF) containing 0.01 M LiBr at a flow rate of 1.0 mL min^{-1} calibrated by standard polystyrene samples. The mechanical properties of bSPPEK membranes were also analyzed by tensile measurement, which was performed with a universal testing instrument (AGS-X 349-05489A, Shimadzu, Japan) at 20 °C and ∼50% RH at a crosshead speed of 2 mm/min. The surface morphology of the membranes was analyzed by an atomic force microscopy (AFM, Dimension Icon, Bruker, USA). Approximately 1 cm^2 of the membranes was cut and equilibrated under 70% RH conditions for at least 24 h before testing. The measurements on ion exchange capacity (IEC), water uptake, and proton conductivity and the atomic simulation methods including free volume calculation, radial distribution function, and diffusion coefficient are referred to in the Supporting Information.

RESULTS AND DISCUSSION

Synthesis of bSPPEKs. The new monomer, bis[5-fluoro-2-(4′-methoxylbenzoyl)]biphenyl (*m*-BFMBP), was prepared in three successive steps, starting with treatment of the raw precursor, 2-chloro-4-fluorobenzoic acid, with thionyl chloride, followed by Friedel−Crafts reaction with anisole, and finally a coupling reaction catalyzed by zerovalent nickel. (See Scheme S1.) Different from our previous report on the synthesis of *p*-BFMBP,[24] the yield of the final *m*-BFMBP monomer was as high as 85% even after a purification step (recrystallization from EtOH). This difference in reaction yields indicates a higher reactivity of the chlorine atom present at the ortho position to the electron-withdrawing group (C═O) than the chlorine at the meta position. The chemical structure of the *m*-BFMBP monomer was elucidated by its ^{13}C−^{1}H COSY NMR spectrum. (See Figure S1.) The typical peak assigned to carbon atom C1 for 2-chloro-4-fluoro-4′-methoxylbenzophenone (CFMP) (δ 129.62) was found to be shifted downfield to 140.96 ppm for *m*-BFMBP, which confirmed the phenyl−phenyl bond formation due to the conjugation effect.

Having confirmed the structure of the *m*-BFMBP monomer, the difluoro- (O1) and diphenoxide- terminated oligomers (O2) were synthesized by coupling either *p*-BFMBP, *m*-BFMBP, or 4,4′-difluorobenzophenone with various bisphenols in the presence of potassium carbonate. Although two of the three bisphenols used in this study are relatively rigid (HQ and BP), the oligomerization reactions proceeded in a homogeneous state. Subsequently, the polycondensation reactions of O1 with O2 were carried out under similar conditions as the oligomerization reactions, to produce the desired multiblock poly(phenylene ether ketone)s (P3) (Scheme 1). The chemical structures of the *meta*-P3 polymers were confirmed by their ^{1}H NMR (Figure 2a) and FTIR spectra. The relative ^{1}H NMR

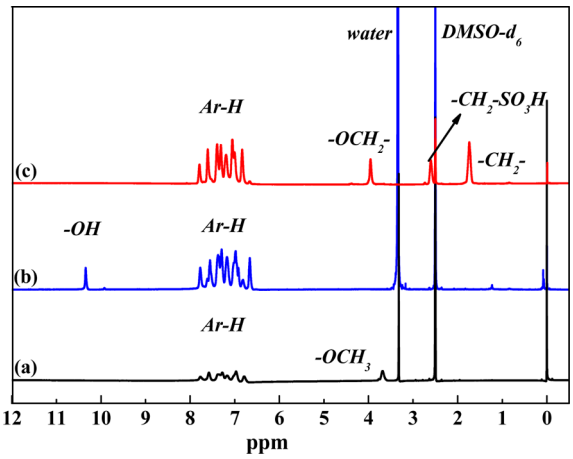

Figure 2. ^{1}H NMR spectrum of (a) P3, (b) P4, and (c) P5. The typical examples were presented from *m*-bSPPEK based on BP type.

signal intensities of the aromatic-H to methoxy-H were around 5.1, 6.2, and 6.1 ppm for *meta*-P3 derived from the three different bisphenols, close to the theoretical values of 5.0 (HQ), 6.3 (BP), and 6.3 ppm (BPE), respectively. Additionally, while comparing the ^{1}H NMR spectrum of *meta*-P3 with that of the starting oligomer O2, the signals assigned to the terminal groups (δ = 6.87 and 6.50 ppm) were absent (Figure S2), suggesting that the target copolymers were formed. The IR spectra of the polymers *meta*-P3 exhibited characteristic absorptions around 2960−2870, 1658, 1597, and 1169 cm^{-1} due to the C−H, C═O, C═C, and C−O−C stretching vibrations, respectively.

The properties of the polymer products are summarized in Table 1. The number-average molecular weights (M_n) and polydispersity indices (PDIs) of P3 were in the range of (4.6−7.6) × 10^4 Da and 2.1−2.5, respectively. Moreover, P3 showed good solubilities in the common organic solvents such as chloroform, dichloromethane, dimethyl sulfoxide, *N*,*N*-dimethylformamide, and so on.

P3 was then converted to P4 by treatment with BBr_3 to carry out the demethylation. Comparing the ^{1}H NMR spectra of *meta*-P3 and *meta*-P4, the characteristic methoxy protons at

DOI: 10.1021/acs.jpcc.5b04480
J. Phys. Chem. C 2015, 119, 19596−19606

Table 1. Physico-Chemical Properties and FFV Data of bSPPEKs

		GPC data[a]			Y^b	E^c	S^d		FFV%		
code	IEC^e	M_n	M_w	PDI	GPa	%	MPa	WU[f]	$\lambda = 1$	$\lambda = 5$	$\lambda = 15$
p-**bSPPEK**-HQ	1.61(1.60)	52	114	2.2	1.30	16	45.3	43	34.7	33.1	31.3
m-**bSPPEK**-HQ	1.61(1.55)	46	105	2.3	0.75	24	38.5	46	35.9	33.2	31.5
p-**bSPPEK**-BP	1.44(1.35)	58	127	2.2	1.12	20	44.7	33	33.3	32.7	30.6
m-**bSPPEK**-BP	1.44(1.34)	60	118	2.0	0.95	33	41.8	40	34.3	32.8	30.5
p-**bSPPEK**-BPE	1.40(1.20)	68	145	2.1	1.10	28	36.9	34	34.6	33.4	30.7
m-**bSPPEK**-BPE	1.40(1.28)	76	190	2.5	0.84	38	33.0	41	35.5	34.0	31.5

[a]kDa. [b]Young's modulus. [c]Elongation. [d]Maximum stress. [e]mequiv g^{-1}, the data and the data in the parentheses refer to the theoretical and titrated *IEC* value, respectively. [f]Water uptake measured at 80 °C, 95% RH.

3.68 ppm of *meta*-P3 were found to have completely disappeared, while hydroxyl proton signals appeared at 10.34 ppm, as shown in Figure 2b. Finally, the bSPPEKs (P5) were obtained by the reaction of the resulting P4 with 1,4-butane sultone in the presence of sodium hydride (Scheme 2).

The chemical structures of the P5 polymers were also confirmed by their FTIR and ^{1}H NMR spectra. The IR spectra of P5 showed characteristic absorptions corresponding to the C═O and C═C stretching around 1658 and 1600 cm^{-1}, whereas the typical O═S═O stretching was observed at around 1119 and 1049 cm^{-1}. The ^{1}H NMR spectra of the P5 polymers are shown in Figure 2c. The new peaks observed at around 3.85 to 4.00 ppm were assigned to the α-methylene protons next to the phenoxyl groups for all three types of P5, indicating the introduction of long sulfoalkyl side chains. Because the typical signals of the α-methylene protons next to the $-SO_3Na$ groups could be easily distinguished near the DMSO-d_6 peak, the ion exchange capacity (IEC_{NMR}) values were then calculated by the relative intensities of the α-methylene protons to the aromatic protons. All of the data obtained were found to be matching well with the theoretical values, which indicates the well-controlled nucleophilic reaction of P4 with 1,4-butane sultone. Additionally, all of the titrated ion exchange capacity (*IEC*) values are close to the theoretical ones for P5, indicating a complete proton exchange process (Table 1).

Physico-Chemical Properties of bSPPEKs. The mechanical properties of all bSPPEKs were determined by a typical tensile stress−strain evaluation procedure, and the data on their Young's modulus (*Y*), maximum stress (*S*), and elongation at break (*E*) values are listed in Table 1. All membranes show good mechanical strength with *Y*, *S*, and *E* values ranging from 0.75 to 1.30 GPa, 16−38 MPa, and 33.0−45.3%, respectively. It should be noted that all of the *m*-bSPPEKs are obtained with somewhat lower *Y* values but greater *S* values than the corresponding *p*-bSPPEKs, which suggests that the *m*-bSPPEKs have more flexible polymer chains.

The morphology of each of the membranes was investigated using a tapping-mode AFM so as to further understand the microphase separation, as shown in Figure 3. Although all of the polymers were based on the block architecture, a more distinct phase separation can be identified in the *m*-bSPPEKs. The *m*-bSPPEKs exhibit clearer and wider clusters compared with *p*-bSPPEKs. The widths of the average hydrophilic domains in *m*-bSPPEKs and *p*-bSPPEKs are about 15−20 and 5−8 nm, respectively. A fairly clear cluster-like morphology is seen in Figure 3f, in which both bright and dark regions are well connected with each other.

Figure S3 displays the proton conductivities of bSPPEKs and Nafion as a function of the relative humidity. Different from most of the aromatic ionomers, *m*-bSPPEKs display a slightly smaller RH dependence than Nafion. When enlarging the region below the 50% RH condition (Figure 4a), some distinguishable characteristics are observed. It is quite encouraging to find that all of the *m*-bSPPEKs (the solid symbol) show greater σ values than the *p*-bSPPEKs under low humidity conditions. Furthermore, it should be noted that *m*-bSPPEK-HQ with an *IEC* of 1.55 mequiv g^{-1} exhibits much higher proton conductivity than Nafion 117, even under low RH conditions. Compared with our previous work,[24] the bSPPEK membranes were obtained with similar good proton conductivities with SPPEs under the same operation condition; however, the *IEC* level is dramatically reduced from a high level of 1.96 to 2.45 to as low as 1.20 to 1.60 mequiv g^{-1}, suggesting a significant improvement on their proton channels.

The relationship between water uptake and proton conductivity of the membranes was investigated, and the results are shown in (Figure 4b), where λ refers to the hydration number. In general, all of the membranes tend to show greater σ with increasing λ values. At each similar λ level, the *m*-bSPPEKs show slightly greater σ values than the *p*-bSPPEKs, and this difference is more evident at a low RH condition of 30%, indicating the much better water-retention capacity of the former polymers. Taking these results into consideration along with the morphological analysis, it is evident that the *m*-bSPPEKs exhibit superior properties as membranes compared with the *p*-bSPPEKs. This is likely due to the more flexible architecture of the *m*-bSPPEKs, which helps in the formation of a more continuous hydrophilic−hydrophobic phase separation, thus improving the ion conduction behavior (Scheme 1). Synthesis of *m*- or *p*-bPPEK (P3): (a) hydroquinone (HQ), (b) 4,4′-biphenol (BP), and (c) 4,4′-oxidiphenol (BPE).

Molecular Dynamic Simulation Analysis of bSPPEKs. It is quite interesting to find that a slight difference in the linkage position of the bSPPEK polymers, resulted in significant differences in their ex situ experimental performance. Therefore, it is important to better understand the structure−property relationship of these polymers to assess the performance changes brought about by structural variations. Herein, we use the two monomer precursors along with the counter monomers of HQ, BP, and BPE to prepare several polymer chains. The repeating unit is set at 10 to 10, with each chain containing 3 hydrophilic and 3 hydrophobic moieties, respectively. In this case, the target molecular weight of the polymers was set at ∼50 kDa, which was close to the experimental M_n values. After several steps of geometry optimization and annealing, the polymer chain was constructed with water molecules into cubic cells under periodic boundary conditions at a temperature of 80 °C. To simulate an actual

DOI: 10.1021/acs.jpcc.5b04480
J. Phys. Chem. C 2015, 119, 19596−19606

Scheme 2. Synthesis of bPPEK−OH (P4) and bSPPEK (P5): (a) Hydroquinone (HQ), (b) 4,4′-Biphenol (BP), and (c) 4,4′-Oxidiphenol (BPE)

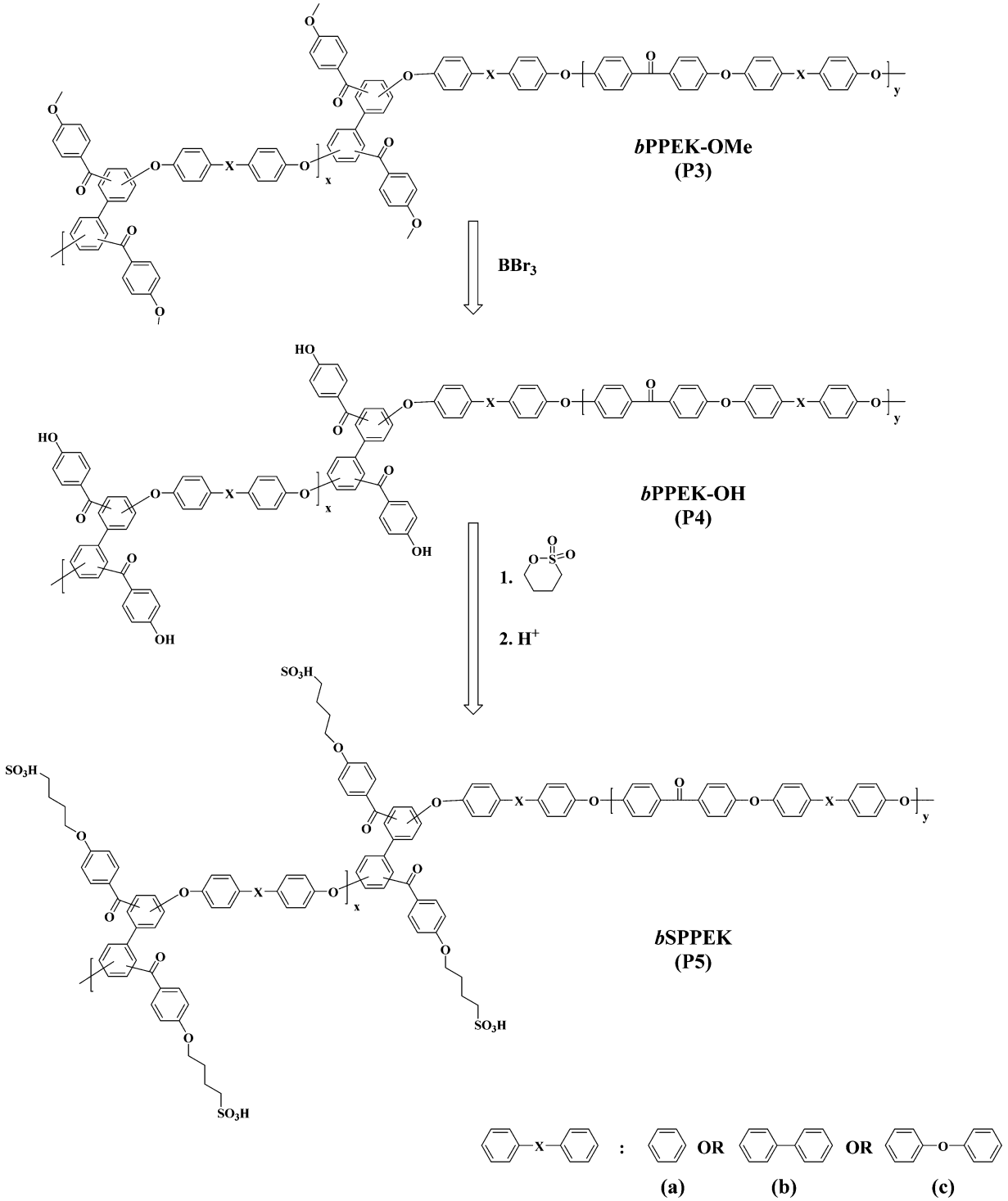

fuel-cell operation situation, water molecules were set with different numbers, that is, λ value equals 1, 5, and 15, which correspond to the relative humidity (RH) conditions of about 30, 50, and 95%, which are the typical RH values used during the fuel-cell operation. (See Figure S4.)

The models were subsequently equilibrated using a COMPASS II force field in several stages. (See Table S1.) After the relaxation process, the constructed models exhibited densities of about 1.22 to 1.38 g cm^{-3} depending on the numbers of water molecules, and the data from the final 1.0 ns were selected for further analysis.

The steric configuration of the bSPPEKs polymers was investigated by tracing the trajectory of the typical atoms or chemical bonds over a simulation period, as shown in Figure 5. The quantity of d is defined as the distance from the "C" in the main chain to the "S" in the sulfonic acid group; θ is defined as the angle between the "C" in the main chain, "C" in the ketone linkage, and "S" in "$-SO_3H$"; and α is the torsion between the

DOI: 10.1021/acs.jpcc.5b04480
J. Phys. Chem. C 2015, 119, 19596−19606

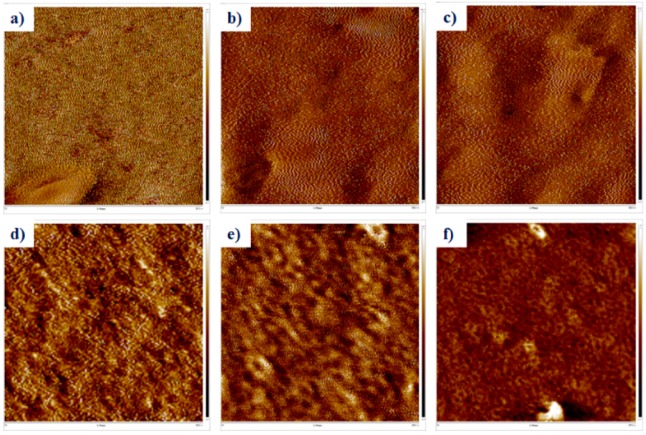

Figure 3. Tapping-mode AFM phase images: (a) *p*-bSPPEK-HQ, (b) *p*-bSPPEK-BP, (c) *p*-bSPPEK-BPE, (d) *m*-bSPPEK-HQ, (e) *m*-bSPPEK-BP, and (f) *m*-bSPPEK-BPE. Scan boxes are 300 × 300 nm.

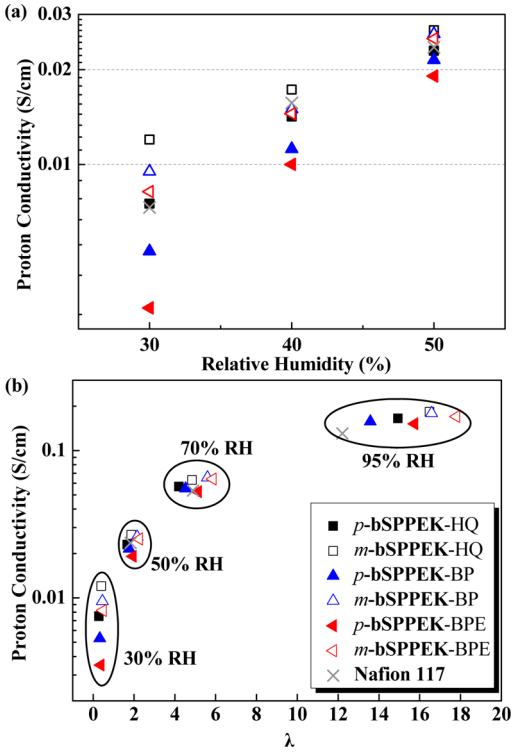

Figure 4. (a) Proton conductivities of bSPPEKs and Nafion 117 as a function of relative humidity conditions (30−50%). (b) Relationship between hydration number (λ) and proton conductivity at 80 °C.

four carbons in the two benzene rings. The trajectory of these bonds, distances, and angles provides valuable information about the steric configuration. It is easy to understand that the larger d means the more extended side chain. Also, the larger θ means the straighter side chain and the larger α means the more coplanar main chain.

The results of lengths, angles and torsion distributions are shown in Figures 6−8. No significant difference could be observed between the p- and m-polymers based on the HQ bisphenol; however, when the BP and BPE type polymers are considered, it can be seen that the side chain of p-polymers exhibits somewhat more flexibility with the peaks shifting to the left, indicating a less extended, curled structure. This is illustrated by the schematic Figure 9a, where $d2$ is greater

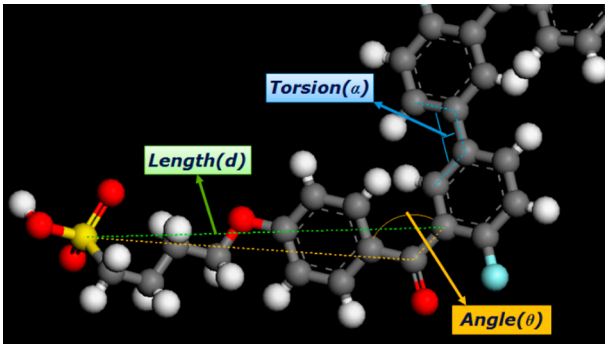

Figure 5. Definition of length (d), angle (θ) and torsion (α) in the model.

than $d1$. Similarly, there is no difference between the HQ and BP types of m- and p-polymers regarding their angle distribution; however, the BPE-type polymer displays opposite contrary trend, where the angle value shifts to the right, indicating a stiff, rod-like architecture. Additionally, all of the *m*-bSPPEKs exhibit some regular and relatively small angles in the main chain, as indicated by the torsion curves. In contrast, the *p*-bSPPEKs are almost all obtained with a coplanar rigid architecture, especially the HQ and BP types.

Taking all of the above results into consideration, it can be seen that the *m*-bSPPEKs show a longer length and smaller angle in the side chain as well as a smaller angle in torsion distribution. A possible reason could be the non-coplanar structure of the *m*-BFMBP monomer itself, which affects the steric hindrance. If the corresponding *meta*-polymer chain could freely move, rotate, and intertwine, coupled to its relatively extended sulfoalkoxyl side chain, there should be more free volume inside the polymer matrix for the *m*-bSPPEKs, just like a set of the skew-hooks, as illustrated in Figure 9a, in contrast with a set of hanging poles for the *p*-bSPPEKs. The higher the free volume, the higher the number of water molecules entering the system, thus resulting in improved ion conduction.

The fractional free volume (FFV) values of the polymers are presented in Table 1. At each hydration level, FFV remains mostly unchanged for the different polymer types; however, it generally decreases with increasing λ values due to swelling. It is well accepted that the addition of highly polar or rigid groups to the aromatic rings of the polymers produces intermolecular interactions,[31,32] and this increased interaction tends to bring molecular segments closer to each other, resulting in a more efficient chain packing and lower FFV; however, when such groups are introduced as rotatable meta linkages into the polymer matrix, they likely take up a lot of space and subsequently cause increase in free volume.[32,33] Therefore, there is a potential trade-off between increasing the chain rigidity and increasing the concentration of bulky m-substituents. It is worth noting that all of the *m*-bSPPEK polymers exhibited a slightly higher FFV than the *p*-bSPPEKs due to the steric bulk of the m-substituents, as previously described. The higher FFV contributes to the better water retention capacity and provides less resistance to the movement of H_2O molecules, both of which are beneficial for the ion migration process.

The coordination numbers (CNs) obtained from the integrations of S−H_2O (H_2O away from the sulfur atom in the sulfonic acid groups) radial distribution functions (RDFs)

DOI: 10.1021/acs.jpcc.5b04480
J. Phys. Chem. C 2015, 119, 19596−19606

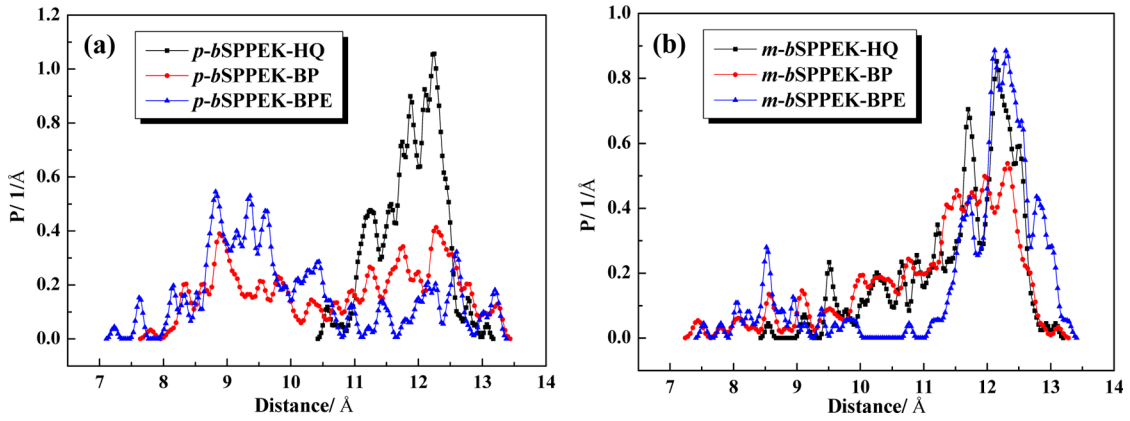

Figure 6. Length distribution of bSPPEKs with varied bisphenol types. The maximum probability correspond to the distance of *ca.* (a) 12.0 Å (HQ), 9.0 Å (BP), and 9.5 Å (BPE) for *p*-bSPPEK, respectively, (b) 12.0 Å (HQ), 12.5 Å (BP), and 12.5 Å (BPE) for *m*-bSPPEK, respectively.

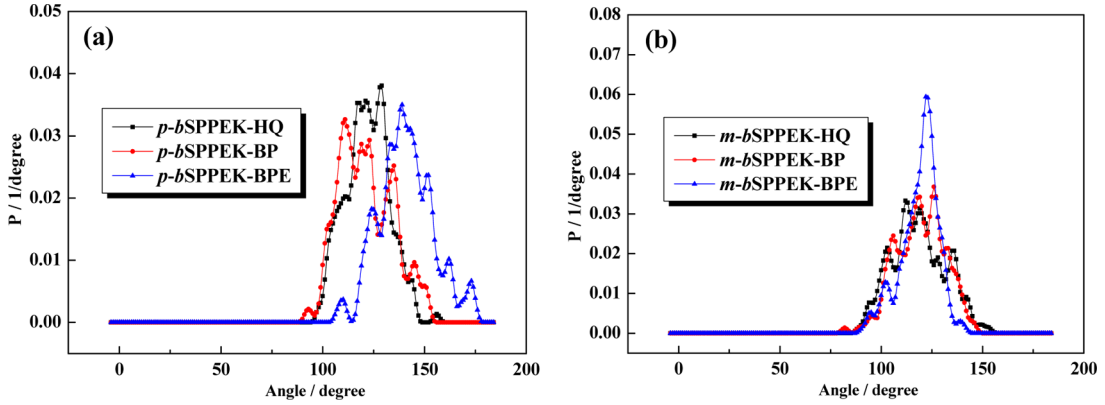

Figure 7. Angle distribution of bSPPEKs with varied bisphenol types. The maximum probability corresponds to the degree of ca. (a) 130° (HQ), 110° (BP), and 140° (BPE) for *p*-bSPPEK, respectively, and (b) 125° (HQ), 110° (BP), and 120° (BPE) for *m*-bSPPEK, respectively.

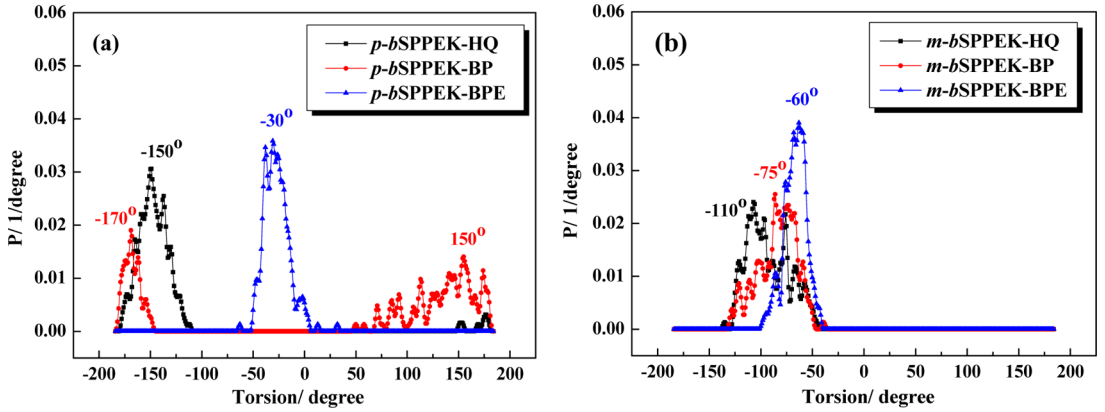

Figure 8. Torsion distribution of bSPPEKs with varied bisphenol types.

provide information about the extent of domain clustering. Figure 9b,c shows the CNs as a function of λ values. In all cases, it can be seen that increasing the hydration level increases the separation, resulting in the enlarged size of the water domain. The RDF curves show that there are two distinct peaks for all of the systems. A sharp peak at ~3.6 Å and a broad peak at ~5.5 Å correspond to the first two hydration shells.[26] By calculating CN at the boundary of 5.5 Å, we found that there is more clustering for the *m*-bSPPEK derived from BPE, with a higher CN (6.5) than that of the corresponding *p*-bSPPEK (6.0), especially under a low RH condition of 30%. Furthermore, the diffusion coefficient (μ) of the water molecules was analyzed by measuring the mean square displacement (MSD) according to Einstein's relation. As shown in Figure 10, all of the *m*-bSPPEKs exhibit greater μ values for H_2O than the *p*-bSPPEKs, which is consistent with our expectation. Therefore, these simulation results are able to explain the observed proton conductive behavior of the two types of bSPPEKs, as previously discussed.

DOI: 10.1021/acs.jpcc.5b04480
J. Phys. Chem. C 2015, 119, 19596−19606

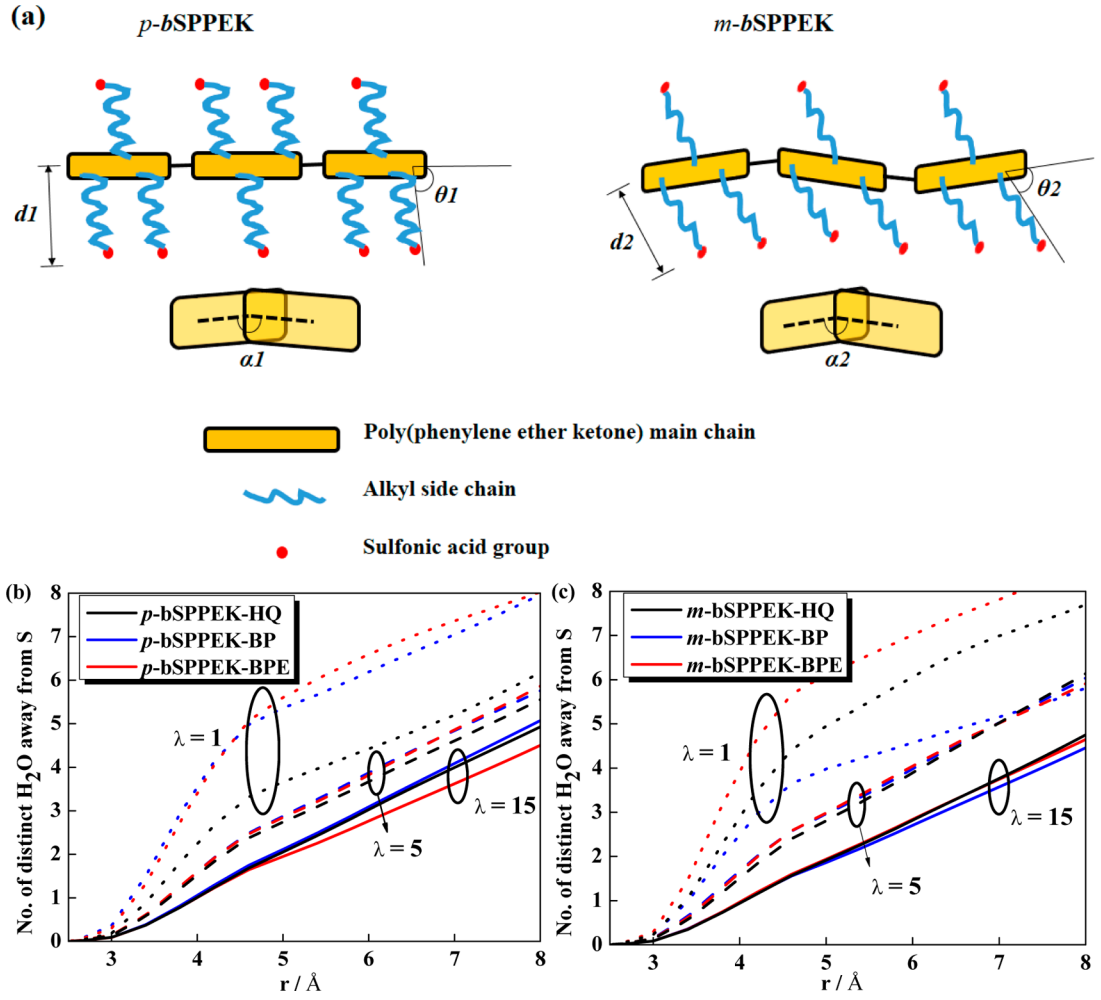

Figure 9. (a) Schematic illustration of bSPPEKs with d, θ, and α, where $d1 < d2$, $\theta1 > \theta2$, and $\alpha1 > \alpha2$. (b,c) Coordination numbers, obtained from integration of the RDFs (Figure S5 and S6), as a function of hydration levels for the distinct H_2O away from sulfur atom at 353 K.

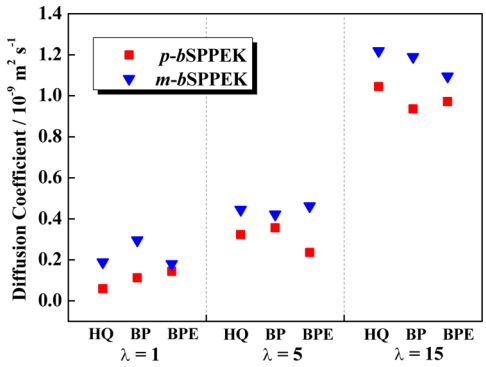

Figure 10. Diffusion coefficient plot of water molecules in the membrane as a function of bisphenol type at λ = 1, 5, and 15 at 353 K.

CONCLUSIONS

Two structural variations of multiblock bSPPEKs with pendant alkylsulfonic acids were prepared by the polycondensation of two difluoro- and diphenoxide-terminated oligomers, and the corresponding free-standing membranes were obtained by the solution casting method. The membranes were found to exhibit acceptable mechanical strength with Y, S, and E values ranging from 0.75 to 1.30 GPa, 16−38 MPa, and 33.0−45.3%, respectively. The meta-isomeric structure was found to have a considerable influence on the electrochemical performance of the multiblock bSPPEKs, and we observed better water-retention capacity for the *m*-bSPPEK, which resulted in its higher proton conductivity. In comparison with the previous work on SPPEs, the bSPPEKs exhibited quite comparable proton conductive behaviors even based on a much lower *IEC* level, suggesting the enhanced aggregation of ion channels. Additionally, AFM images of the *m*-bSPPEKs showed clear microphase separation, which provides further evidence of understanding the ion transport behavior. The steric configuration obtained from the molecular dynamics simulation clearly revealed that the *m*-SPPEKs have a longer length and smaller angle for the side chain as well as a small angle for the polymer main chain compared with the *p*-SPPEKs, which suggests a bulky structure of the former. Meanwhile, the increase in main-chain flexibility is largely responsible for the greater FFV values for the *m*-SPPEKs, which helped the proton migration behavior. In general, the simulation results showed good consistency with the experimental results and helped to provide a good explanation for the proton conductive properties of the two types of bSPPEKs. Thus, it is clear that from this work that *m*-bSPPEKs have valuable potential for application in a fuel-cell system.

DOI: 10.1021/acs.jpcc.5b04480
J. Phys. Chem. C 2015, 119, 19596−19606

■ ASSOCIATED CONTENT

Supporting Information

The Supporting Information is available free of charge on the ACS Publications website at DOI: 10.1021/acs.jpcc.5b04480.

Atomistic simulation including the model establishment, equilibration and dynamic steps, and radial distribution function. Characterization data of bSPPEKs. (PDF)

■ AUTHOR INFORMATION

Corresponding Authors

*X.Z.: E-mail: xuanzhang@mail.njust.edu.cn.
*M.U.: E-mail: ueda.m.ad@m.titech.ac.jp.
*L.W.: E-mail: wanglj@njust.edu.cn.

Notes

The authors declare no competing financial interest.

■ ACKNOWLEDGMENTS

This work was financially supported by the NSFC (21406117), the Natural Science Foundation of Jiangsu Province (BK20140782), National Science Foundation for Postdoctoral Scientists of China (2014M561652), the Jiangsu Planned Projects for Postdoctoral Research Funds (1401045B), Scientific Research Foundation for Returned Scholars (Ministry of Education of China), PAPD, the Fundamental Research Funds for the Central Universities (30920140122008), and Industrial Technology Research Grant Program in 2011 (#11B02008c) from NEDO of Japan.

■ REFERENCES

(1) Dunn, B.; Kamath, H.; Tarascon, J.-M. Electrical Energy Storage for the Grid: A Battery of Choices. *Science* **2011**, *334*, 928−935.

(2) Li, N.; Guiver, M. D. Ion Transport by Nanochannels in Ion-Containing Aromatic Copolymers. *Macromolecules* **2014**, *47*, 2175−2198.

(3) Kreuer, K.-D. Ion Conducting Membranes for Fuel Cells and other Electrochemical Devices. *Chem. Mater.* **2014**, *26*, 361−380.

(4) Liu, Y.-L. Developments of highly proton-conductive sulfonated polymers for proton exchange membrane fuel cells. *Polym. Chem.* **2012**, *3*, 1373−1383.

(5) Zhang, H.; Shen, P. K. Recent Development of Polymer Electrolyte Membranes for Fuel Cells. *Chem. Rev.* **2012**, *112*, 2780−2832.

(6) Yandrasits, M.; Hamrock, S. Poly(perfluorosulfonic acid) Membranes. In *Polymer Science: A Comprehensive Reference*; Elsevier: Amsterdam, The Netherlands, 2012.

(7) Li, Q.; Chen, Yu.; Rowlett, J. R.; McGrath, J. E.; Mack, N. H.; Kim, Y. S. Controlled Disulfonated Poly(Arylene Ether Sulfone) Multiblock Copolymers for Direct Methanol Fuel Cells. *ACS Appl. Mater. Interfaces* **2014**, *6* (8), 5779−5788.

(8) Takamuku, S.; Jannasch, P. Multiblock Copolymers with Highly Sulfonated Blocks Containing Di- and Tetrasulfonated Arylene Sulfone Segments for Proton Exchange Membrane Fuel Cell Applications. *Adv. Energy Mater.* **2012**, *2* (1), 129−140.

(9) Miyatake, K.; Hirayama, D.; Bae, B.; Watanabe, M. Block poly(arylene ether sulfone ketone)s containing densely sulfonated linear hydrophilic segments as proton conductive membranes. *Polym. Chem.* **2012**, *3* (9), 2517−2522.

(10) Miyake, J.; Watanabe, M.; Miyatake, K. Sulfonated Poly(arylene ether phosphine oxide ketone) Block Copolymers as Oxidatively Stable Proton Conductive Membranes. *ACS Appl. Mater. Interfaces* **2013**, *5* (13), 5903−5907.

(11) Zhang, X.; Higashihara, T.; Ueda, M.; Wang, L. Polyphenylenes and the related copolymer membranes for electrochemical device applications. *Polym. Chem.* **2014**, *5* (21), 6121−6141.

(12) He, Q.; Xu, T.; Qian, H.; Zheng, J.; Shi, C.; Li, Y.; Zhang, S. Enhanced proton conductivity of sulfonated poly(p-phenylene-co-aryl ether ketone) proton exchange membranes with controlled microblock structure. *J. Power Sources* **2015**, *278*, 590−598.

(13) Zhang, X.; Sheng, L.; Higashihara, T.; Ueda, M. Polymer electrolyte membranes based on poly(m-phenylene)s with sulfonic acid via long alkyl side chains. *Polym. Chem.* **2013**, *4*, 1235−1242.

(14) Wang, C.; Shin, D. W.; Lee, S. Y.; Kang, N. R.; Robertson, G. P.; Lee, Y. M.; Guiver, M. D. A clustered sulfonated poly(ether sulfone) based on a new fluorene-based bisphenol monomer. *J. Mater. Chem.* **2012**, *22*, 25093−25101.

(15) Zhang, X.; Hu, Z.; Pu, Y.; Chen, S.; Ling, J.; Bi, H.; Chen, S.; Wang, L.; Okamoto, K. Preparation and properties of novel sulfonated poly(p-phenylene-co-aryl ether ketone)s for polymer electrolyte fuel cell applications. *J. Power Sources* **2012**, *216*, 261−268.

(16) Umezawa, K.; Oshima, T.; Yoshizawa-Fujita, M.; Takeoka, Y.; Rikukawa, M. Synthesis of Hydrophilic−Hydrophobic Block Copolymer Ionomers Based on Polyphenylenes. *ACS Macro Lett.* **2012**, *1*, 969−972.

(17) Li, N.; Lee, S. Y.; Liu, Y. L.; Lee, Y. M.; Guiver, M. D. A new class of highly-conducting polymer electrolyte membranes: Aromatic ABA triblock copolymers. *Energy Environ. Sci.* **2012**, *5* (1), 5346−5355.

(18) Zhang, X.; Hu, Z.; Luo, L.; Chen, S.; Liu, J.; Chen, S.; Wang, L. Graft-crosslinked Copolymers Based on Poly(arylene ether ketone)-gc-sulfonated Poly(arylene ether sulfone) for PEMFC Applications. *Macromol. Rapid Commun.* **2011**, *32* (14), 1108−1113.

(19) Si, K.; Dong, D.; Wycisk, R.; Litt, M. Synthesis and characterization of poly(para-phenylene disulfonic acid), its copolymers and their n-alkylbenzene grafts as proton exchange membranes: high conductivity at low relative humidity. *J. Mater. Chem.* **2012**, *22*, 20907−20917.

(20) Liao, H.; Zhang, K.; Tong, G.; Xiao, G.; Yan, D. Sulfonated poly(arylene ether phosphine oxide)s with various distributions and contents of pendant sulfonic acid groups synthesized by direct polycondensation. *Polym. Chem.* **2014**, *5* (2), 412−422.

(21) Zhang, X.; Chen, S.; Liu, J.; Hu, Z.; Chen, S.; Wang, L. Preparation and properties of sulfonated poly(phenylene arylene)/sulfonated polyimide (SPA/SPI) blend membranes for polymer electrolyte membrane fuel cell applications. *J. Membr. Sci.* **2011**, *371* (1−2), 276−285.

(22) Chang, Y.; Brunello, G.; Fuller, J.; Disabb-Miller, M. L.; Hawley, M. E.; Kim, Y. S.; Hickner, M. A.; Jang, S. S.; Bae, C. Polymer electrolyte membranes based on poly(arylene ether sulfone) with pendant perfluorosulfonic acid. *Polym. Chem.* **2013**, *4* (2), 272−281.

(23) Pang, J.; Feng, S.; Yu, Y.; Zhang, H.; Jiang, Z. Poly(aryl ether ketone) containing flexible tetra-sulfonated side chains as proton exchange membranes. *Polym. Chem.* **2014**, *5* (4), 1477−1486.

(24) Zhang, X.; Sheng, L.; Hayakawa, T.; Ueda, M.; Higashihara, T. Polymer electrolyte membranes based on poly(phenylene ether)s with sulfonic acid via long alkyl side chains. *J. Mater. Chem. A* **2013**, *1* (37), 11389−11396.

(25) Giffin, G. A.; Haugen, G. M.; Hamrock, S. J.; Di Noto, V. Interplay between Structure and Relaxations in Perfluorosulfonic Acid Proton Conducting Membranes. *J. Am. Chem. Soc.* **2013**, *135* (2), 822−834.

(26) Tse, Y. L. S.; Herring, A. M.; Kim, K.; Voth, G. A. Molecular Dynamics Simulations of Proton Transport in 3M and Nafion Perfluorosulfonic Acid Membranes. *J. Phys. Chem. C* **2013**, *117* (16), 8079−8091.

(27) Wu, D.; Paddison, S. J.; Elliott, J. A. A comparative study of the hydrated morphologies of perfluorosulfonic acid fuel cell membranes with mesoscopic simulations. *Energy Environ. Sci.* **2008**, *1* (2), 284−293.

(28) Jorn, R.; Voth, G. A. Mesoscale Simulation of Proton Transport in Proton Exchange Membranes. *J. Phys. Chem. C* **2012**, *116* (19), 10476−10489.

(29) Wu, D.; Paddison, S. J.; Elliott, J. A.; Hamrock, S. J. Mesoscale Modeling of Hydrated Morphologies of 3M Perfluorosulfonic Acid-Based Fuel Cell Electrolytes. *Langmuir* **2010**, *26* (17), 14308−14315.

DOI: 10.1021/acs.jpcc.5b04480
J. Phys. Chem. C 2015, 119, 19596−19606

(30) Ishimoto, T.; Nagumo, R.; Ogura, T.; Ishihara, T.; Kim, B.; Miyamoto, A.; Koyama, M. Chemical Degradation Mechanism of Model Compound, $CF_3(CF_2)_3O(CF_2)_2OCF_2SO_3H$, of PFSA Polymer by Attack of Hydroxyl Radical in PEMFCs. *J. Electrochem. Soc.* **2010**, *157* (9), B1305−B1309.
(31) Wang, F.; Hickner, M.; Kim, Y. S.; Zawodzinski, T. A.; McGrath, J. E. Direct polymerization of sulfonated poly(arylene ether sulfone) random (statistical) copolymers: candidates for new proton exchange membranes. *J. Membr. Sci.* **2002**, *197*, 231−242.
(32) Xie, W.; Ju, H.; Geise, G. M.; Freeman, B. D.; Mardel, J. I.; Hill, A. J.; McGrath, J. E. Effect of Free Volume on Water and Salt Transport Properties in Directly Copolymerized Disulfonated Poly(arylene ether sulfone) Random Copolymers. *Macromolecules* **2011**, *44*, 4428−4438.
(33) Ayala, D.; Lozano, A. E.; Abajo, J.; Perez, C. G.; Campa, J. G.; Peinemann, K. V.; Freeman, B. D.; Prabhakar, R. Gas separation properties of aromatic polyimides. *J. Membr. Sci.* **2003**, *215*, 61−73.

DOI: 10.1021/acs.jpcc.5b04480
J. Phys. Chem. C 2015, 119, 19596−19606